

## Supporting Information

### Sulfur Oxidation Mediated Controllable Reconstruction on $\text{LiCo}_{1.9}\text{Fe}_{0.1}\text{O}_4$ for Boosted Electrochemical Water Oxidation

Bing Xiong<sup>1</sup>, Haige Tan<sup>1</sup>, Yangkai Wang<sup>1</sup>, Tian Sang<sup>1</sup>, Weiwei Li<sup>1</sup>, Jianlin Wang<sup>2</sup>, Qiuping Huang<sup>2</sup>, Na Li<sup>2</sup>, Zhengping Fu<sup>1,2\*</sup>, Yalin Lu<sup>1,2\*</sup>

<sup>1</sup> Department of Materials Science and Engineering, Key Laboratory of Precision and Intelligent Chemistry, University of Science and Technology of China, Hefei 230026, China

<sup>2</sup> Anhui Laboratory of Advanced Photon Science and Technology, Synergetic Innovation Center of Quantum Information & Quantum Physics, Hefei National Research Center for Physical Sciences at the Microscale, University of Science and Technology of China, Hefei 230026, China

#### Methods

##### Materials synthesis

All chemical reagents used in this work were analytical grade without further purification.

**Synthesis of spinel oxides:** The spinel  $\text{LiCo}_2\text{O}_4$  (LCO) and  $\text{LiCo}_{1.9}\text{Fe}_{0.1}\text{O}_4$  (LCFO) were synthesized by a modified sol-gel combustion method. First,  $\text{LiNO}_3$ ,  $\text{Co}(\text{NO}_3)_2 \cdot 6\text{H}_2\text{O}$ , and  $\text{Fe}(\text{NO}_3)_3 \cdot 9\text{H}_2\text{O}$  with a specific molar ratio were dissolved in the diluted nitric acid solution under vigorous stirring. Citric acid (used as chelating agent) was added into the solution. The resulting mixture was then stirred at 80 °C for several hours until it transforms into a viscous gel. The gel was dried in air at 170 °C for 12 hours and then ground thoroughly. Finally, the resulting powder was heated at 450 °C (ramp rate 2 °C/min) for 12 h to obtain pure phase spinel oxides. Note:  $\text{Fe}(\text{NO}_3)_3 \cdot 9\text{H}_2\text{O}$  is not required for the synthesis of LCO.

**Sulfurization process:** Taking LCFO as an example, the typical sulfurization details are as follows. For LCFO-01, 0.1 g as-prepared LCFO powder was placed at the lower air outlet and 0.1 g sulfur powder was placed at the upper air outlet of a tube furnace and heated at 300 °C (ramp rate 5 °C/min) for 2 h under argon atmosphere. The resulting product was named LCFO-01.

For LCFO-02, the sulfurization process was the same as that of LCFO-01, except that 0.2 g sulfur powder was used.

For LCFO-03, the sulfurization process was the same as that of LCFO-01, except that 0.3 g sulfur powder was used, and the heating process was extended to 4 h.

The sulfurization process of LCO was the same as that of LCFO.

##### Synthesis of $\text{Co}_{0.95}\text{Fe}_{0.05}\text{S}_2$ :

The  $\text{Co}_{0.95}\text{Fe}_{0.05}\text{S}_2$  precursors are synthesized by hydrothermal method. 1.9 mM (mM)  $\text{Co}(\text{NO}_3)_2 \cdot 6\text{H}_2\text{O}$ , 0.1 mM, 4 mM  $\text{NH}_4\text{F}$ , and 10 mM urea were mixed in 60 mL deionized water under magnetic stirring. Then, the mixtures were transferred into a Teflon stainless-steel autoclave, heating at 110 °C for 5 h. The obtained products were cleaned and dried in a vacuum oven at 60 °C to form the precursors. Finally, 0.05 g precursor powders and 0.2 g sulfur powder were placed in a tube furnace and heated at 300 °C (ramp rate 5 °C/min) for 2 h under argon atmosphere.

##### Characterization

X-ray diffraction (XRD) curves of catalysts were acquired on four-circle diffractometer at a scanning rate of 10 °min<sup>-1</sup> (Rigaku, SmartLab, Cu  $K_\alpha$  radiation). Renishaw inVia Raman microscope with an excitation source of 532-nm laser and coupled with a 50 telephoto objective lens (Leica) was conducted to record Raman spectra. X-ray photoelectron spectroscopy (XPS) profiles were performed using ESCALAB 250 with Al- $K_\alpha$  irradiation.

---

Soft X-ray absorption spectra (XAS) were collected at the BL12B-a facility of the National Synchrotron Radiation Laboratory (NSRL, HeFei, P.R. China). Scanning electron microscopy (SEM, Hitachi-SU8220) and high-resolution transmission electron microscopy (HRTEM, JEOL JEM-2100 plus, 200kV) were carried out to obtain the morphological information of the catalysts.

### **Electrochemical measurements**

All the electrochemical measurements were performed at room temperature on CHI 760E. The oxygen evolution reaction (OER) analysis was testing in a conventional three-electrode cell with a glassy carbon electrode (diameter: 3 mm) as the working electrode, platinum wire as the counter electrode, and KCl-saturated Ag/AgCl as the reference electrode. The working electrode was prepared as follows: 5 mg catalyst were mixed with 1 mg acetylene black (AB), then dispersed in 500  $\mu\text{L}$  water/isopropanol ( $v/v = 3:1$ ) solvent followed by the addition of 50  $\mu\text{L}$  Nafion solution as the binder. The mixtures were ultrasonicated for 1 h to reach homogeneous ink, 3  $\mu\text{L}$  of the ink was taken and spread onto the surface of the glassy carbon electrode to yield a final mass loading of  $0.386 \text{ mg cm}^{-2}$ . Different electrolytes, containing 1 M KOH, and 1 M KOH with different addition of  $\text{K}_2\text{SO}_4$  were used.

### **Calculations**

The spin-polarized density functional theory (DFT) calculations<sup>1, 2</sup> were carried out in the Vienna ab initio simulation package (VASP) based on the plane-wave basis sets with the projector augmented-wave method<sup>3, 4</sup>. The exchange-correlation potential was treated by using a generalized gradient approximation (GGA) with the Perdew-Burke-Ernzerhof (PBE) parametrization<sup>5</sup>. The energy cutoff was set to be 400 eV. The Brillouin-zone integration was sampled with a  $\Gamma$ -centered Monkhorst-Pack mesh<sup>6</sup> of  $2 \times 2 \times 1$  by VASPKIT<sup>7</sup>. The structures were fully relaxed until the maximum force on each atom was less than  $0.05 \text{ eV}/\text{\AA}$ , and the energy convergent standard was  $10^{-4} \text{ eV}$ . The van der Waals correction of Grimme's DFT-D3 model was also adopted<sup>6</sup>. To avoid the periodic interactions for interface structures, a vacuum layer as large as 15  $\text{\AA}$  is used along the  $c$  direction normal to the interface. The relevant computational formulas for the oxygen evolution reaction and the S oxidation reaction can be found in reference<sup>7</sup>.

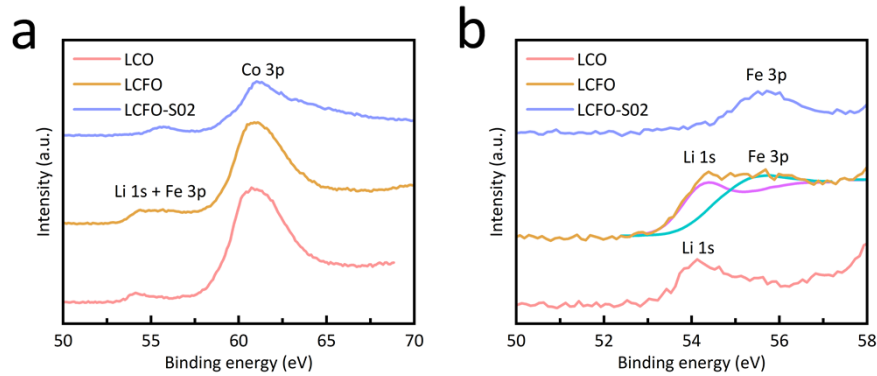


Figure S1. (a) High-resolution Li 1s XPS spectra. (b) The enlarged Li 1s XPS spectra. Discussion 1: From the spectra in Figure S1a, the peaks situate at 61 eV can be ascribed to the Co 3p signal.<sup>8</sup> In the enlarged spectra (Figure S1b), the peaks locate at 54.2 eV and 55.7 eV correspond to the Li 1s and Fe 3p signals, respectively.<sup>9</sup> The Li 1s peaks in LCO and LCFO confirm the successful introduction of the Li element in the as-prepared spinel oxides. And the negligible Li 1s signal in LCFO-S02 is attributed to the formation of sulfide shell on the surface of the catalyst.

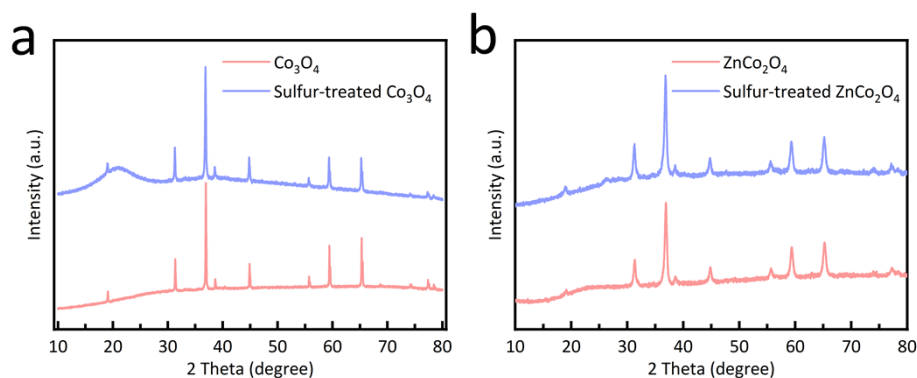


Figure S2. (a) XRD patterns of Co<sub>3</sub>O<sub>4</sub> and sulfurization-treated Co<sub>3</sub>O<sub>4</sub>. (b) XRD patterns of ZnCo<sub>2</sub>O<sub>4</sub> and sulfurization-treated ZnCo<sub>2</sub>O<sub>4</sub>.

Discussion2: The XRD patterns of the sulfur-treated Co<sub>3</sub>O<sub>4</sub> and ZnCo<sub>2</sub>O<sub>4</sub> match well with their pristine counterparts, which suggest the maintained spinel structure in the sulfurization process. Actually, sulfur doped Co<sub>3</sub>O<sub>4</sub> and ZnCo<sub>2</sub>O<sub>4</sub> with stabilized spinel structure have been widely reported to be used as catalysts.<sup>10-13</sup>

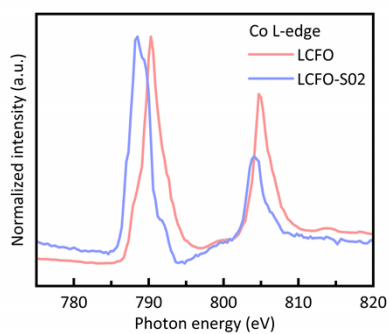


Figure S3. Normalized Co L-edge soft X-ray adsorption spectra.

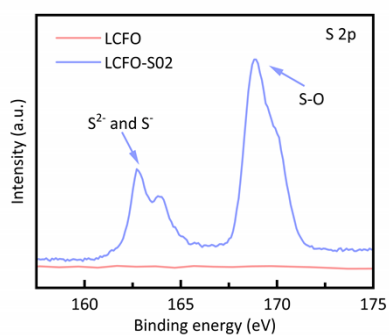


Figure S4. S 2p XPS spectra of LCFO and LCFO-S02.

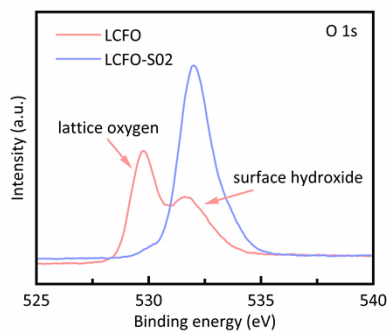


Figure S5. O 1s XPS spectra of LCFO and LCFO-S02.

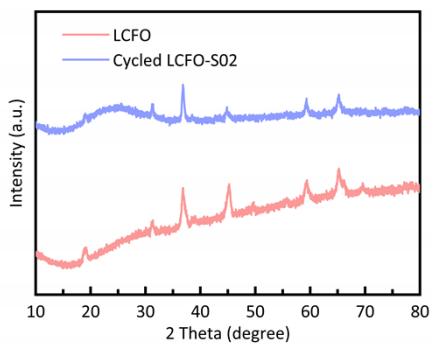


Figure S6. XRD patterns of LCFO and cycled LCFO-S02.

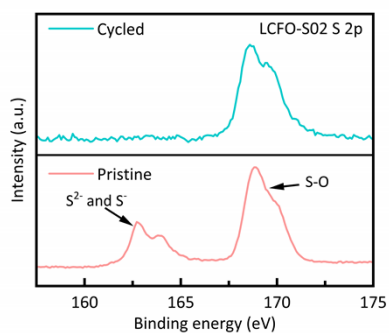


Figure S7. S 2p XPS spectra of pristine and cycled LCFO-S02.

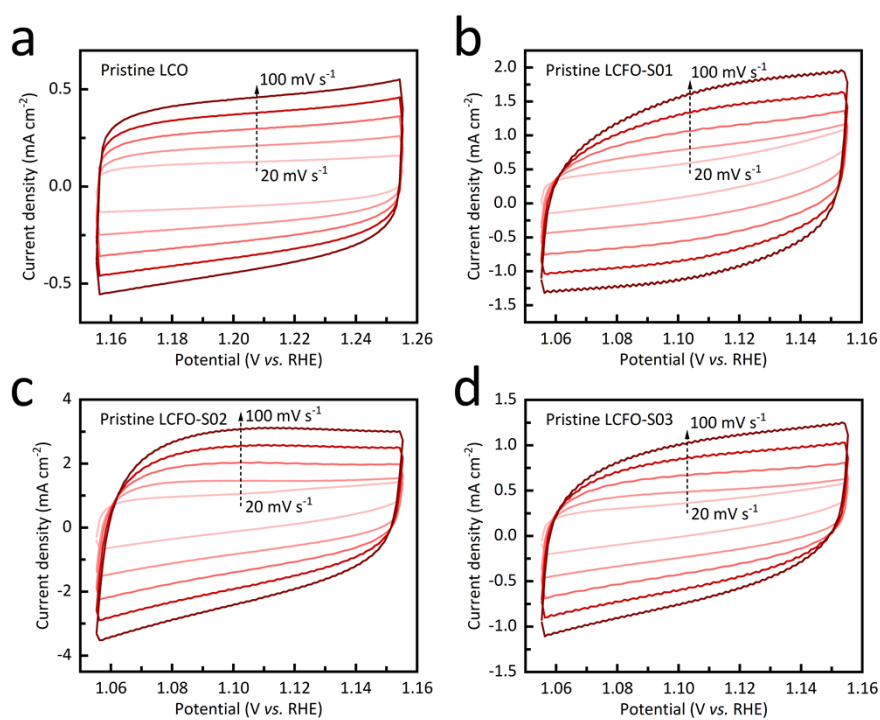


Figure S8. CV curves of the pristine catalysts recorded in the non-Faradaic region in 1 M KOH.

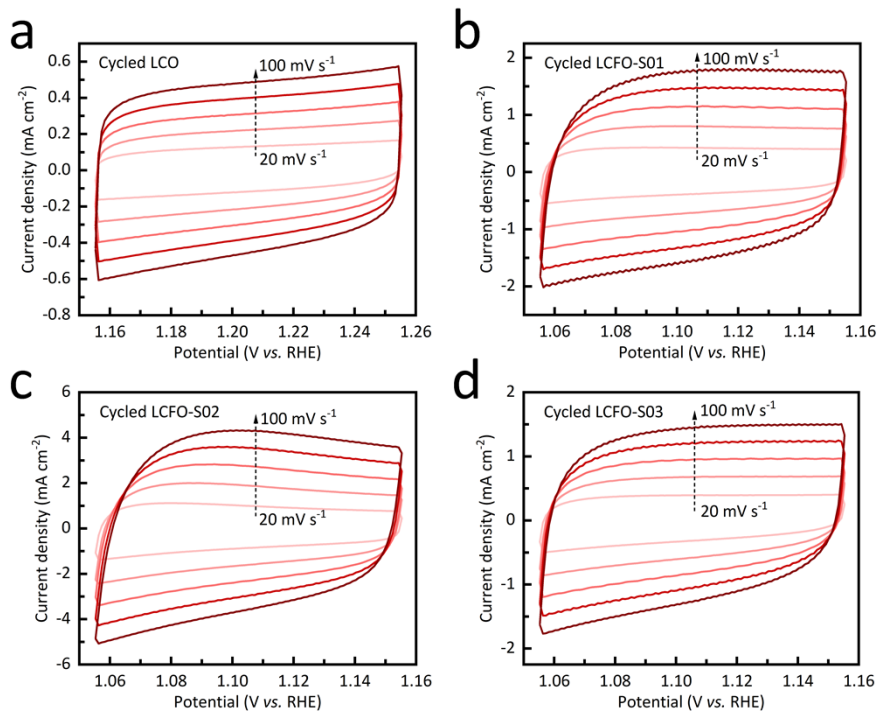


Figure S9. CV curves of the cycled catalysts recorded in the non-Faradaic region in 1 M KOH.

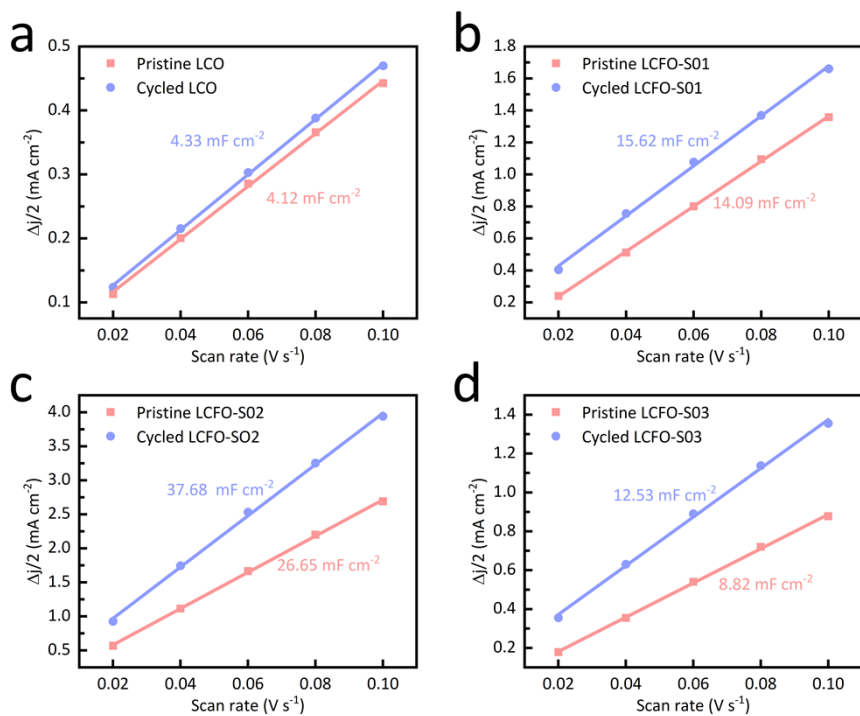


Figure S10. The linear fittings of the capacitive currents versus CV scans.

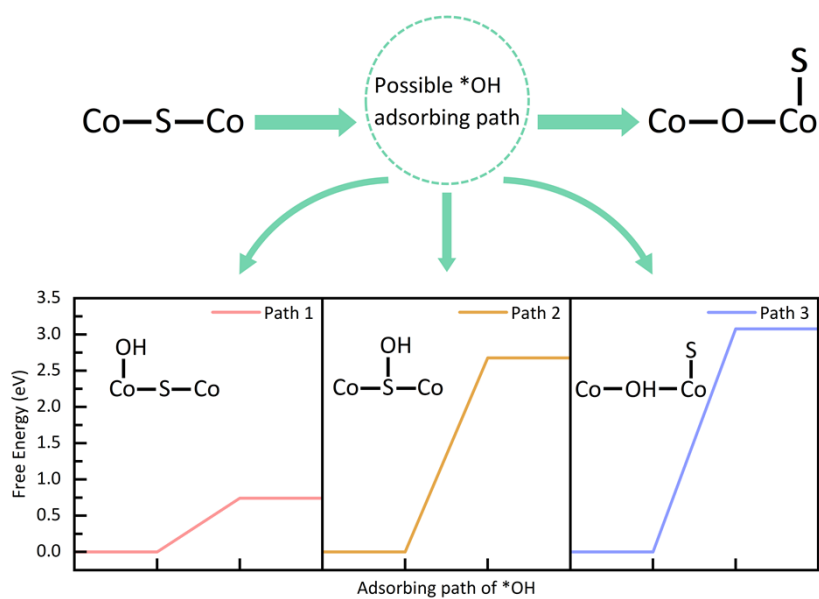


Figure S11. Three possible reaction pathways and Gibbs free energy of S-leaching.

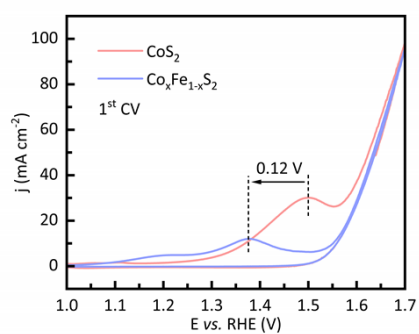


Figure S12. The 1<sup>st</sup> CV curves of  $\text{CoS}_2$  and  $\text{Co}_x\text{Fe}_{1-x}\text{S}_2$ .

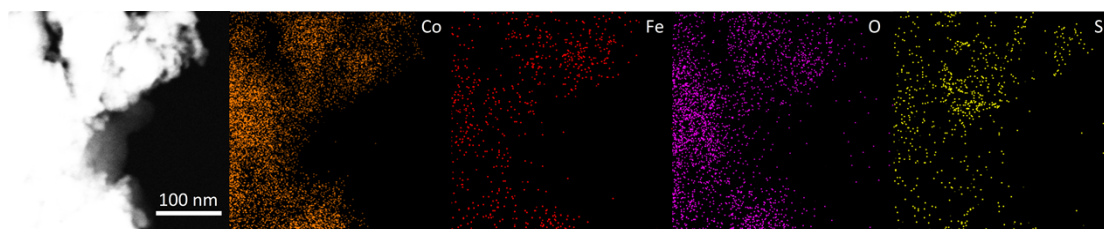


Figure S13. The TEM-EDS mapping of the cycled LCFO-S02. The spectroscopy proves that the material surface contains sulfur components, corresponding to the surface-adsorbed  $\text{SO}_4^{2-}$ .

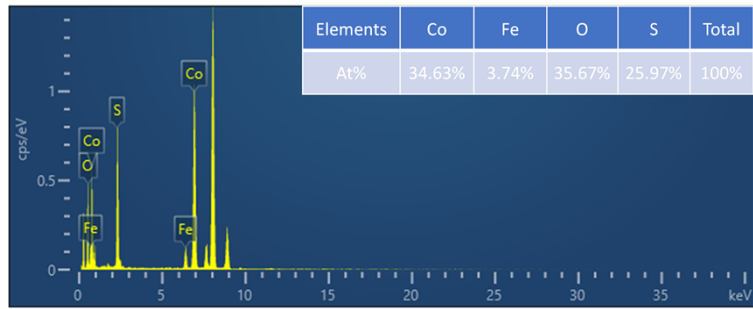


Figure S14. The EDS profile of pristine LCFO-S02.

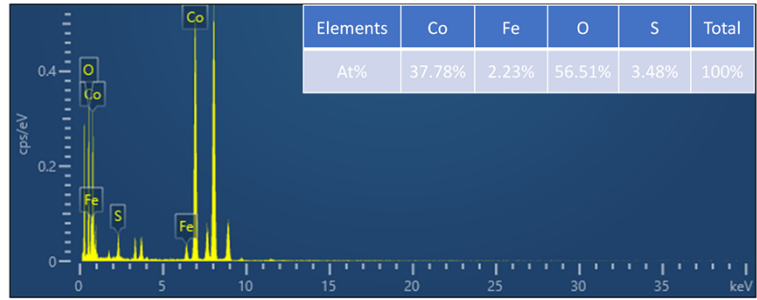


Figure S15. The EDS profile of cycled LCFO-S02.

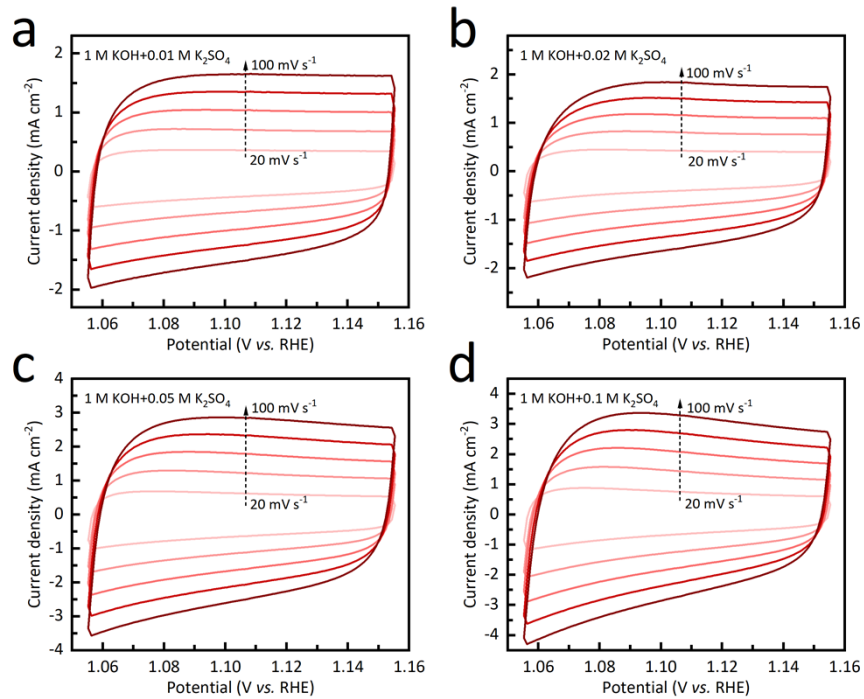


Figure S16. The CV curves in different electrolytes: 1 M KOH+0.01 M K<sub>2</sub>SO<sub>4</sub> (a); 1 M KOH+0.02 M K<sub>2</sub>SO<sub>4</sub> (b); 1 M KOH+0.05 M K<sub>2</sub>SO<sub>4</sub> (c); 1 M KOH+0.1 M K<sub>2</sub>SO<sub>4</sub> (d).



Table S1 The S 2p XPS spectra area obtained from the integration.

Catalysts	Species	Area	
LCFO-S01	S <sup>2+</sup> /S <sup>-</sup>	22272.4	37.2%
	S-O	37533.6	62.8%
LCFO-S02	S <sup>2+</sup> /S <sup>-</sup>	24547.7	40%
	S-O	36844	60%
LCFO-S03	S <sup>2+</sup> /S <sup>-</sup>	27755.1	43.1%
	S-O	36595.8	56.9%

## References

1. P. Hohenberg and W. Kohn, *Physical Review*, 1964, **136**, B864-B871.
2. W. Kohn and L. J. Sham, *Physical Review*, 1965, **140**, A1133-A1138.
3. G. Kresse and J. Furthmüller, *Physical Review B*, 1996, **54**, 11169-11186.
4. P. E. Blöchl, *Physical Review B*, 1994, **50**, 17953-17979.
5. J. P. Perdew, K. Burke and M. Ernzerhof, *Physical Review Letters*, 1997, **78**, 1396-1396.
6. F. Ortmann, F. Bechstedt and W. G. Schmidt, *Physical Review B*, 2006, **73**, 205101.
7. W. Wang, A. Wang, J. Xu, H. Li, M. Yu, A. Dong, Z. Li, C. Zhao, F. Cheng and W. Wang, *Journal of Colloid and Interface Science*, 2024, **657**, 334-343.
8. X. Liu, Y. Tan, W. Wang, C. Li, Z. W. Seh, L. Wang and Y. Sun, *Nano Letters*, 2020, **20**, 4558-4565.
9. N. Luo, Y. Lin, J. Guo, E. Quattrocchi, H. Deng, J. Dong, F. Ciucci, F. Boi, C. Hu and S. Grasso, *Materials*, 2021, **14**, 2826.
10. X. Chen, X. Wang, D. Jiang, F. Xie, K. Xie and Y. Wang, *Journal of Alloys and Compounds*, 2020, **831**, 154772.
11. T. Jiang, N. Yin, Z. Bai, P. Dai, X. Yu, M. Wu and G. Li, *Applied Surface Science*, 2018, **450**, 219-227.
12. B. Xiong, L. Ge, X. Lei, Y. Wang, J. Yang, W. Li, X. Li, Z. Cheng, Z. Fu and Y. Lu, *Science China Materials*, 2023, **66**, 1793-1800.
13. Y. Yang, C. Yang, K. Tao, Q. Ma and L. Han, *Vacuum*, 2020, **181**, 109740.